단순지지와 자유의 방사연단을 갖는 단순지지 부채꼴형 평판의 휨진동

Flexural Vibrations Of Simply Supported Sectorial Plates with Simply Supported And Free Radial Edges

한봉구* 김주우**

Han Bong-Koo Kim, Joo-Woo

요 지

본 논문에서는 원형연단이 단순지지 되어 있을 때 단순과 자유의 방사연단 조건을 갖는 부채꼴형 평판의 휨진동에 대한 엄밀한 해석방법을 제시한다. Ritz방법을 이용하여 수직진동변위를 두가지 적합 함수식으로 가정하였다. 이러한 두가지의 적합 함수식은 (1) 수학적으로 완전한 대수 삼각다항함수와, (2) 둔각 모서리에서의 휨모멘트 특이도를 고려하는 모서리함수로 구성되어있다. 본 연구에서는 방사연단의 둔각 모서리를 이루는 부채꼴형 각도의 범위에 따른 엄밀한 진동수 및 수직진동 변위의 전형적인 등고선을 제시하였다.

Key words : ritz method, classical plate theory, vibration, stresses, corner stress singularities, sectorial plate, bending, natural frequencies

1. INTRODUCTION

Accumulated in the literature for nearly two centuries are approximately 200 technical publications explaining the free vibration characteristics of complete circular and annular plates with various support conditions along the circumferential boundaries or at interior points. The scope of previous work done for the sectorial plate (see Fig. 1), in comparison, is quite narrow. Several authors have offered approximate theoretical and experimental vibration data for thin sectorial and annular sector plates with various edge conditions on the circular and radial edges[(1), (2), (3), (4)].

The present work examines sectorial plates having a simply supported circumferential edge, and a simply supported and free radial edge (SFS; see Fig. 1, wherein those edges which are simply supported and free have been

* 정회원, 서울산업대학교 구조공학과 부교수

** 서울산업대 구조공학과 강사

● 본 논문에 대한 토의를 1999년 2월 28일까지 학회로 보내주시면 1999년 4월호 토론결과를 게재하겠습니다.

identified by letters S and F), including stress singularity effects at the sharp vertex corner. For a very small notch angle, 360° $-\alpha$ (say, one degree or less), a deep hinged and free radial crack ensues. A Ritz procedure is employed, which incorporates a complete set of admissible algebraic-trigonometric polynomials in conjunction with an admissible set of corner functions that exactly model the singular vibratory moments which exist at the vertices of corner angles (α) which exceed 128 degrees[5]. The first set guarantees convergence to exact frequencies as sufficient terms are retained.

The second set substantially accelerates the convergence of frequencies, which is demonstrated through an convergence study summarized herein.

Accurate nondimensional frequencies are presented as the corner angle α is varied. To better understand the nature of the stress singularities existing in the title problem, normalized contour plots of the vibratory transverse displacements are studied for plates having sector angles α = 90^0, 180^0, (semi-circular), 270^0, 300^0, 330^0, 355^0, and 360^0 (sharp radial crack).

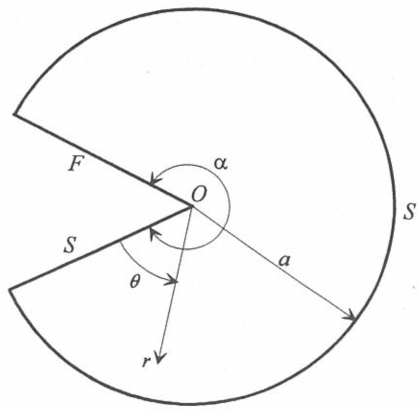

Fig. 1. Geometric description of a SFS sectorial plate

2. METHODOLOGY

Consider the polar coordinates (r, θ) originating at the vertex of the sectorial plate of radius, a, shown in Fig. 1. The transverse vibratory displacement w is defined in terms of these coordinates as follows:

$$W(r, \theta, t) = W(r, \theta) \sin \omega t, \tag{1}$$

where t is time and ω is the circular frequency of vibration.

Displacement trial functions are assumed as the sum of two finite sets: $W = W_p + W_c$, where W_p is algebraic-trigonometric polynomial and W_c is corner function. The admissible polynomial for a SFS sectorial plate is written as

$$W_p = g(r, \theta)\Big(\sum_{m=0,2,4}^{M_1} \sum_{n=0,2,4}^{m} A_{mn}\, r^m \cos n\theta + \sum_{m=1,3,5}^{M_2} \sum_{n=1,3,5}^{m} A_{mn}\, r^m \cos n\theta + \sum_{m=2,4}^{M_3} \sum_{n=2,4}^{m} B_{mn}\, r^m \sin n\theta + \sum_{m=1,3,5}^{M_4} \sum_{n=1,3,5}^{m} B_{mn}\, r^m \sin n\theta \Big), \tag{2}$$

in which

$$g(r, \theta) = (r/a)^2 (\theta/\alpha)(a^2 - r^2). \tag{3}$$

In Eq. (2), A_{mn} and B_{mn} are arbitrary coefficients, and the values of m and n have been specially chosen to eliminate those terms which yield undesirable singularities at r=0, and yet, preserve the mathematical completeness of the resulting series as sufficient terms are retained. Thus, convergence to the exact frequencies is guaranteed when the series is employed in the present Ritz procedure.

The displacement polynomial Eq. (2) should, in principle, yield accurate frequencies. However, the number of terms required may be computationally prohibitive. This problem is alleviated by augmentation of the displacement polynomial trial set with admissible *corner functions*, which introduce the proper singular vibratory moments at the vertex corner formed by the radial edges (Fig. 1). The set of corner functions is taken as

$$W_c = G(r) \sum_{k=1}^{K} C_k W^*_{c_k}, \tag{4}$$

where C_k are arbitrary coefficients, and $W^*_{c_k}$, are solutions of the fourth-order biharmonic, static equilibrium equation for bending of plates at acute corner angles(5).

$$W^*_{c_k} = r^{\lambda_k+1}[\, a_k \sin(\lambda_k+1)\theta + b_k \cos(\lambda_k+1)\theta + c_k \sin(\lambda_k-1)\theta + d_k \cos(\lambda_k-1)\theta]. \tag{5}$$

The essential boundary conditions along the radial edge $\theta = 0$ is simply supported [*i.e.*, $W(r,0) = M_r(r,0) = 0$] and $\theta = \alpha$ is free [*i.e.*, $V_r(r, \alpha) = M_r(r, \alpha) = 0$] (see Fig. 1), where M_r and V_r are the usual radial moment and shear force defined elsewhere(6). These conditions are used in Eq. (5) to construct a set of algebraic equations from which the values λ_k are obtained as roots of the vanishing determinants. Thus, satisfaction of the simply supported-free (S-F) radial edge conditions results in the following characteristic equation for the λ_k,

$$\sin 2\lambda_k \alpha = \frac{\nu - 1}{3+\nu} \lambda_k \sin 2\alpha. \tag{6}$$

The corresponding corner function is

$$W^*_{c_k}(r, \theta) = r^{\lambda_k+1}[\sin(\lambda_k+1)\theta - \gamma_{1_k}\cos(\lambda_k+1)\theta - \gamma_{2_k}\sin(\lambda_k-1)\theta + \gamma_{3_k}\cos(\lambda_k-1)\theta], \tag{7}$$

where

$$\gamma_{1_k} = \frac{\sin(\lambda_k+1)\alpha/2}{\cos(\lambda_k+1)\alpha/2}, \tag{8a}$$

$$\gamma_{2_k} = \frac{(\lambda_k+1)(\nu-1)\sin(\lambda_k+1)\alpha/2}{[\lambda_k(\nu-1)+(3+\nu)]\sin(\lambda_k-1)\alpha/2}, \tag{8b}$$

$$\gamma_{3_k} = \frac{(\lambda_k+1)(\nu-1)\sin(\lambda_k+1)\alpha/2}{[\lambda_k(\nu-1)+(3+\nu)]\cos(\lambda_k-1)\alpha/2}. \tag{8c}$$

For the simply supported circumferential edge, the boundary function $G(r) = (a^2 - r^2)$ in Eq. (4). Some of λ_k the obtained from Eq. (6) may be complex numbers, and thus, result in complex corner functions. In such cases, both the real and imaginary parts are used as independent functions in the present Ritz procedure.

In employing the Ritz method for free

vibration problems, one has to construct the following frequency equations which are

$$\frac{\partial(V_{max}-T_{max})}{\partial A_{mn}}=0,$$
$$\frac{\partial(V_{max}-T_{max})}{\partial B_{mn}}=0, \qquad (9)$$
$$\frac{\partial(V_{max}-T_{max})}{\partial C_{k}}=0,$$

In Eqs. (9), the maximum strain energy, Vmax, in the plate due to bending in a vibratory cycle is

$$V_{max}=\frac{D}{2}\int_A\{D[(\chi_r+\chi_\theta)^2-2(1-\nu)(\chi_r\chi_\theta-\chi_{r\theta}^2)]dA \qquad (10)$$

where $dA = rdrd\theta$, $D=Eh^3/12(1-\nu)$ is flexural rigidity, h is the plate thickness, E is Young's modulus, ν is Poisson's ratio, and χ_r, χ_θ, and $\chi_{r\theta}$ are the maximum bending and twisting curvatures:

$$\chi_r=\frac{\partial^2W}{\partial r^2},\quad \chi_\theta=\frac{1}{r}\frac{\partial W}{\partial r}+\frac{1}{r^2}\frac{\partial^2W}{\partial\theta^2},$$
$$\chi_{r\theta}=\frac{\partial}{\partial r}\left(\frac{1}{r}\frac{\partial W}{\partial\theta}\right). \qquad (11)$$

The maximum kinetic energy is

$$T_{max}=\frac{\rho\omega^2}{2}\int_A W^2dA, \qquad (12)$$

in which ρ is the mass per unit area of the plate. The required area integrals in the dynamical energy Eqs. (10) and (12) are performed numerically.

Substituting Eqs. (2)-(4), (7), and (8) into (9)-(12) yields a set of homogeneous algebraic equations involving the coefficients A_{mn}, B_{mn}, and C_k. The roots of the vanishing determinant of these equations are a set of eigenvalues, which are expressed in terms of the non-dimensional frequency parameter $\omega a^2(\rho/D)^{1/2}$ commonly used in the plate vibration literature. Eigenvectors involving the coefficients Amn, Bmn, and C_k are determined in the usual manner by substituting the eigenvalues back into the homogeneous equations. Normalized contours of the associated mode shapes may be depicted on a $r-\theta$ grid in the sector plate domain, once the eigenvectors are substituted into Eqs. (2) and (4).

3. CONVERGENCE STUDIES

Having outlined the Ritz procedure employed in the present analysis, it is now appropriate to address the important question of convergence rate of frequencies, as various numbers of algebraic-trigonometric polynomials and corner functions are retained. All of the frequency and mode shape data shown in the present and following sections are for materials having a Poisson's ratio (ν) equal to 0.3.

Summarized in Table 1 is the first six non-dimensional frequencies $\omega a^2(\rho h/D)^{1/2}$ for a SFS sectorial plate with α = 330^0. As indicated in Table 1, the lowest frequency mode of the plate exhibits a slow upper bound monotonic decrease of $\omega a^2(\rho h/D)^{1/2}$ to an inaccurate value of 12.925, as the number of polynomial terms (W_p) is increased with no corner functions. That is, the polynomial series, albeit complete, is converging very slowly. An examination of the next five rows of data reveals that an accurate value to five significant figures is 12.447. Interestingly, a trial set consisting of a single corner function

Table 1. Convergence of frequency parameters $\omega a^2(\rho/D)^{1/2}$ for a sectorial plate having simply supported-free radial edges and simply supported circumferential edge (α = 330^0)

Mode no.	No. of corner functions	Total number of terms in Wp			
		46	60	84	112
1	0	13.215	13.080	12.987	12.925
	1	12.986	12.835	12.729	12.658
	5	12.504	12.482	12.467	12.459
	10	12.454	12.451	12.449	12.448
	15	12.450	12.449	12.448	12.447
	20	12.449	12.448	12.448	12.447
2	0	16.399	16.061	15.850	15.700
	1	16.029	15.758	15.581	15.453
	5	14.195	14.176	14.165	14.159
	10	14.147	14.147	14.147	14.146
	15	14.147	14.147	14.146	14.146
	20	14.147	14.147	14.146	14.146
3	0	21.290	20.503	20.007	19.664
	1	17.436	17.314	17.254	17.224
	5	17.215	17.179	17.157	17.145
	10	17.137	17.134	17.132	17.131
	15	17.133	17.132	17.131	17.131
	20	17.132	17.131	17.131	17.131
4	0	25.435	24.929	24.585	24.347
	1	24.929	24.579	24.333	24.162
	5	23.503	23.484	23.471	23.465
	10	23.466	23.462	23.459	23.458
	15	23.460	23.459	23.458	23.457
	20	23.458	23.458	23.458	23.457
5	0	35.168	33.237	32.322	31.813
	1	35.147	33.234	32.321	31.810
	5	30.804	30.715	30.666	30.640
	10	30.628	30.619	30.614	30.612
	15	30.612	30.611	30.610	30.610
	20	30.610	30.610	30.610	30.610
6	0	39.573	39.145	38.925	38.801
	1	39.554	39.133	38.921	38.800
	5	38.606	38.567	38.555	38.549
	10	38.575	38.547	38.543	38.541
	15	38.546	38.542	38.540	38.540
	20	38.542	38.540	38.540	38.540

(corresponding to the lowest λ_k) along with a smaller number of 84 polynomial terms yields an upper bound value of 12.729 which is slightly lower than the 12.925 value obtained with 112 polynomial terms and no corner functions. With larger trial sets of 84 polynomials and 10 corner functions, four significant figure convergence of the lowest frequency mode is achieved. One can clearly see that by adding the first 20 corner functions to as few as 40 polynomials yields the value of 12.449, which is exact to four significant figures.

4. FREQUENCY AND MODE SHAPES

Convergence studies were performed to compile in Table 2 the least upper bound frequency parameters $\omega a^2(\rho h/D)^{1/2}$ for the first six modes of a SFS sectorial plate with increasing sector angles α = 90^0, 180^0, 270^0, 300^0, 330^0, 350^0, 355^0, and 360^0. All frequency results are guaranteed upper bounds to exact values (typically accurate to the five significant figures shown in Table 2). Hence, Table 2 provides an accurate database of frequencies for the SFS sectorial plates having various corner

Table 2. Frequency parameters $\omega a^2(\rho/D)^{1/2}$ for sectorial plates having simply supported-free radial edges and simply supported circumferential edge

α (degrees)	Mode number					
	1	2	3	4	5	6
90	12.498	34.872	45.608	68.868	86.609	98.448
180	11.989	18.022	30.269	44.265	45.254	56.285
270	13.358	13.672	20.368	28.696	38.228	47.212
300	12.758	13.840	18.555	25.763	33.954	43.035
330	12.447	14.146	17.131	23.457	30.610	38.540
350	12.391	14.291	16.329	22.177	28.760	36.044
355	12.393	14.321	16.144	21.883	28.337	35.474
360	12.405	14.373	15.968	21.600	27.928	34.924

angles against which future results using experimental or theoretical methods (such as finite element analysis) may be compared. Generally speaking, it is clear in Table 2 that $\omega a^2(\rho h/D)^{1/2}$ decreases as the sector angle α increases. Slight exceptions to this trend is shown in the first and second modes of the plate.

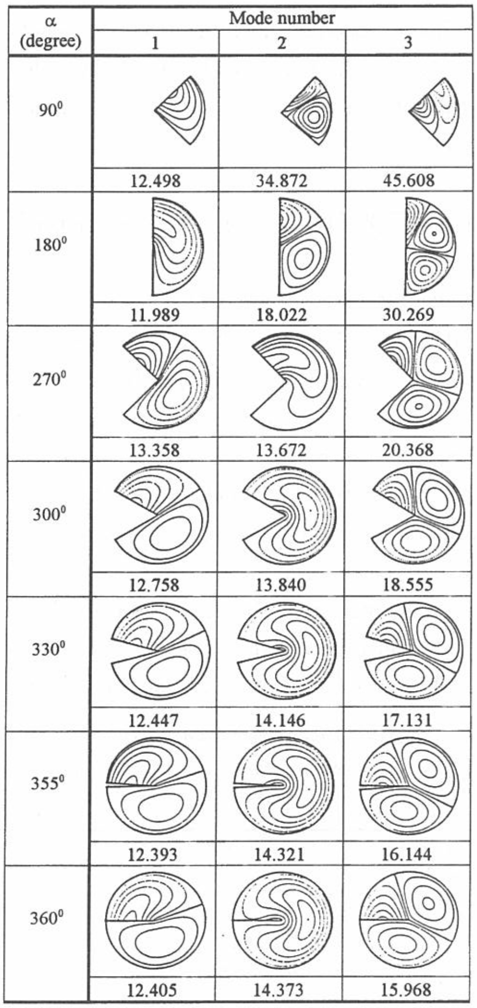

Fig. 2 Normalized Transverse displacement contours (W/W_{max}) for a sectorial plate having simply supported-free radial edges and simply supported circumferential edge

Shown in Fig. 2 are normalized transverse displacement contours for the first three modes of the SFS sectorial plates for α = 90^0, 180^0, 270^0, 300^0, 330^0, 355^0, and 360^0. These contour plots are normalized with respect to the maximum transverse component (*i.e.*, $-1 \leq W/ W_{max} \leq 1$, where the negative values of W/Wmax are depicted as dashed contour lines in Fig. 2, and non-dimensional frequencies shown correspond to the data listed in Table 2). Contour lines are shown for W/Wmax = ± 0.2, ± 0.4, ± 0.6, ± 0.8, ± 1. Nodal patterns of each mode are shown in Fig. 2 as darker contour lines of zero displacement (W/W_{max} = 0) during a vibratory motion.

Given the absence of symmetry in the SFS displacement contours (see Fig. 2), their nodal patterns are rotated slightly in the clockwise direction. It is interesting to note that the fundamental mode shapes for $\alpha \geq 270^0$ have one nodal line, which is nearly radial, whereas the second mode shapes have none.

5. CONCLUDING REMARKS

Highly accurate frequencies and mode shapes for sectorial plates with a simply supported circumferential edge and a simply supported and free radial edge have been obtained using a Ritz procedure in conjunction with classical thin-plate theory. In this approximate procedure, the assumed transverse displacement of the plate constitutes a hybrid set of complete algebraic-trigonometric polynomials along with corner functions that account for singular bending moments at the vertex of acute corner angle.

Numerical table has been presented,

showing the variations of non-dimensional frequencies (accurate to at least five significant figures) over a spectra of vertex angles α. A primal conclusion explicating the title problem is that the large bending moment stresses in the neighborhood of the vertex of simply supported and free radial edge of vibrating sectorial plate do indeed significantly influence the frequencies.

REFERENCES

1. Bhattacharya, A. P. and Bhowmic, K. N., Free vibration of a sectorial plate, Journal of Sound and Vibration, Vol. 41, No. 4, pp. 503-505, 1975.
2. Rubin, C., Nodal circles and natural frequencies for the isotropic wedge, Journal of Sound and Vibration, Vol. 39, No. 4, pp. 523-526, 1975.
3. Maruyama, K. and Ichinomiya, O., Experimental investigation of free vibrations of clamped sector plates, Journal of Sound and Vibration, Vol. 74, No. 4, pp. 563-573, 1981.
4. Kim, C. S., and Dickinson, S. M., On the free, transverse vibration of annular and circular, thin, sectorial plates subjected to certain complicating effects, Journal of Sound and Vibration, Vol. 134, pp. 407-421, 1989.
5. Williams, M. L., Surface stress singularities resulting from various boundary conditions in angular corners of plates under bending, Proceedings of the First U.S. National Congress of Applied Mechanics, pp. 325-329, 1951.
6. Leissa, A. W., Vibration of Plates, NASA SP-160. Washington, D.C.: U.S. Government Printing Office, 1969. (Reprinted by The Acoustical Society of America, 1993).

(접수일자 : 98.11.12)